

# Data-Driven Worker Activity Recognition and Picking Efficiency Estimation in Manual Strawberry Harvesting

---

Uddhav Bhattarai<sup>1,\*</sup>, Rajkishan Arikapudi<sup>1</sup>, Steven A. Fennimore<sup>2</sup>, Frank N Martin<sup>3</sup>,  
Stavros G. Vougioukas<sup>1,\*</sup>

<sup>1</sup>Department of Biological and Agricultural Engineering, University of California, Davis, CA, 95616, USA

<sup>2</sup>Department of Plant Sciences, University of California, Davis, CA, 95616, USA

<sup>3</sup>Crop Improvement and Protection Research Unit, U.S. Department of Agriculture Agricultural Research Service, Salinas, CA 93905, USA

\*Corresponding authors: ubhattarai@ucdavis.edu, svougioukas@ucdavis.edu

## Abstract

Manual fruit harvesting is common in agriculture, but the amount of time that pickers spend on nonproductive activities can make it very inefficient. Accurately identifying picking vs. non-picking activity is crucial for estimating picker efficiency and optimizing labor management and the harvest process. In this study, a practical system was developed to calculate the efficiency of pickers in commercial strawberry harvesting. Instrumented picking carts were used to record in real-time the harvested fruit weight, geo-location, and cart movement. A fleet of these carts was deployed during the commercial strawberry harvest season in Santa Maria, CA. The collected data was then used to train a CNN-LSTM-based deep neural network to classify a picker’s activity into “Pick” and “NoPick” classes. Experimental evaluations showed that the CNN-LSTM model showed promising activity recognition performance with an F1 score accuracy of up to 0.974. The classification results were then used to compute two worker efficiency metrics: the percentage of time spent actively picking, and the time required to fill a tray. Analysis of the season-long harvest data showed that the pickers spent an average of 73.56% of their total harvest time actively picking strawberries, with an average tray fill time of 6.22 minutes. The mean accuracies of these metrics were 96.29% and 95.42%, respectively. When integrated on a

commercial scale, the proposed technology could aid growers in automated worker activity monitoring and harvest optimization, ultimately helping to reduce non-productive time and enhance overall harvest efficiency.

**Keywords:** picker activity recognition, CNN-LSTM model, picker efficiency estimation, harvest monitoring, IoT in agriculture, precision agriculture, harvest optimization

## 1 Introduction

Most fresh-market fruits and vegetables are still harvested manually. However, manual harvesting is highly labor-intensive and costly, and the available farm labor workforce has not been able to meet the grower needs (Bratt, 2015; Hubbart, 2020). Despite advances in robotic harvesting of fruits and vegetables such as strawberries (Xiong et al., 2020), apples (Zhang et al., 2024), and sweet peppers (Arad et al., 2020), most harvesting robots are still in the prototyping phase and cannot match or exceed manual labor in terms of reliability, cost, speed, and scalability. Growers continue to depend on manual labor for harvesting. Improved labor management and work efficiency could reduce the dependence on labor. However, current methods for quantifying worker efficiency depend on manual observations, such as counting the number of harvested trays or bags per hour or shift. This approach is not scalable, and fails to track the temporal dynamics of picker activities. As a result, it is difficult to track the significant amount of time pickers spend on non-productive tasks, such as transporting full containers, waiting in queues for delivery, and repositioning in the field to continue harvesting.

Despite potential practical applications, activity recognition has often been overlooked in agricultural contexts. Current activity recognition methods utilize either images or time series data, such as acceleration readings. With advancements in Convolutional Neural Networks (CNNs), the accuracy and robustness of vision-based activity recognition methods have significantly improved. Pal et al. (2023) developed a Mask R-CNN and Optical flow-based machine vision approach for human activity classification in agriculture. However, agricultural workers operate in cluttered environments characterized by frequent occlusions and diverse worker motions, posing challenges in identifying pickers, tracking them, and recognizing their activities throughout the harvest period. Therefore, it is more practical to develop systems based on direct measurement by sensors that can capture harvest-related signals, such as harvested mass, or picker location or travel speed. Recently, researchers have developed systems such as instrumented picking carts (Anjom

et al., 2018), instrumented picking bags (Fei et al., 2020), and wearable sensors (Dabrowski and Rahman, 2023) to measure real-time harvest data and monitor picker motion. While the picking cart developed by Anjom et al. (2018) and picking bag developed by Fei et al. (2020) record harvest mass, acceleration, and location, they were primarily integrated into harvest assist systems rather than for activity recognition or efficiency evaluation. The wearable sensor developed by Dabrowski and Rahman (2023) was designed to detect bag-emptying events during manual avocado harvesting but did not identify the picker’s picking activity or estimate picker efficiency.

Recognizing picking activities during manual harvest is challenging since the picking data is embedded within a complex mix of non-picking activities throughout the harvest period. During manual harvest, each picker is provided with picking carts and trays with clamshells for placing fruits like strawberries or larger bags or buckets for apples or avocados. When a tray or bag is full, the pickers move to a designated collection point, often located at the edge of the field or within the rows. If a picker reaches the end of a row with a partially full container, they typically move to a new unharvested row to resume picking. The harvest data contains data-related activities such as active picking, traveling to a collection station for fruit delivery, returning to rows to restart harvesting, switching rows to continue harvesting, as well as idle time before and after harvest and during the breaks. Furthermore, since pickers manually handle the sensing modules, the collected data gets heavily noisy because of the variation in handling, making the activity recognition and efficiency computation challenging.

The main goal of this study was to develop a robust data-driven approach to identify active picking events during manual harvest and estimate and evaluate picker efficiency. To achieve this goal instrumented picking carts (iCarritos) were developed and deployed during commercial strawberry harvest in California, USA. The picking carts were equipped with two load cells, a Global Navigation Satellite System (GNSS) receiver, and an Inertial Measurement Unit (IMU) to record harvested fruit weight, geolocation, and cart motion data. To identify active picking events, a robust Convolutional Neural Network - Long Short-Term Memory (CNN-LSTM) based deep learning algorithm was developed that classifies raw harvest data into picking and non-picking ( “Pick” and “NoPick”) classes. The picker efficiency was then evaluated as the percentage of time spent actively picking over the entire harvest period and the amount of time spent by pickers to fill up a tray. The following are the main contributions of the paper:

- Picker efficiency during manual harvest was estimated and evaluated using instrumented picking carts and a robust deep learning-based activity recognition algorithm.

- Extensive harvest data was collected during the commercial harvest, and the dataset with annotations was made publicly available for further research in this area.

The remaining sections of this paper are organized as follows. Section 2 details the data collection process, proposed CNN-LSTM-based activity recognition algorithm, and the picker efficiency estimation process and discusses the metrics to evaluate the accuracy of picker activity recognition and efficiency estimation. Section 3 evaluates the accuracy of activity recognition and efficiency estimation algorithm followed by picker efficiency estimation in season-long harvest data. Finally, Section 4 concludes the paper by summarizing the key findings and their implications.

## 2 Materials and Methods

### 2.1 Data Collection

Data was collected from instrumented picking carts (iCarrito) consisting of two load cells and a GNSS unit with onboard IMU that measured real-time harvest mass, cart location, and motion (see Figure 1). A Raspberry Pi 0W (Raspberry Pi Foundation, UK) microcomputer with an SD card was used to run the carrito software and store the harvest data. The GNSS unit, the Piksi Multi (Swift Navigation Inc., USA), was a low-cost GPS system that used corrections from the freely available Satellite-Based Augmentation System (SBAS). The GNSS unit has a rated horizontal Circular Error Probable (CEP) accuracy of 0.75 meters. The harvest data was recorded at 10 Hz with information on Raspberry Pi Unix timestamp, GNSS Unix timestamp, GNSS time of week (*ms*), latitude (*degrees*), longitude (*degrees*), height (*m*), acceleration in x-axis ( $m/s^2$ ), acceleration in y-axis ( $m/s^2$ ), acceleration in z-axis ( $m/s^2$ ), raw mass (*Kg*). Additionally, the bed center locations were collected using RTK GPS to geolocate the harvest row and field boundary accurately.

The iCarritos were deployed during commercial strawberry harvest in Santa Maria, CA, for the entire harvest season spanning 27 harvest days (April 10, 2024 - July 17, 2024) with 752 iCarrito deployments. Data collected from early to peak harvest season, covering 12 harvest days (April 10, 2024 - May 25, 2024), were utilized to train and evaluate the activity recognition model and picker efficiency estimation. Data from the entire harvest season was analyzed for a more comprehensive estimation of picker efficiency.

Figure 2 shows the recorded mass and acceleration data by iCarrito during a typical harvest day. The

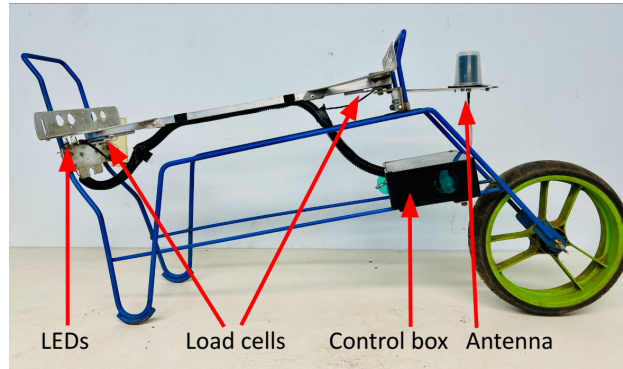


Figure 1: Instrumented picking cart (iCarrito) developed by instrumenting traditional wire frame structure picking carts (Carrito). It consists of two load cells, a SwiftNav Piksi Multi GNSS unit, a control box with Raspberry Pi 0W microcomputer and SD card, control switches, and status LEDs.

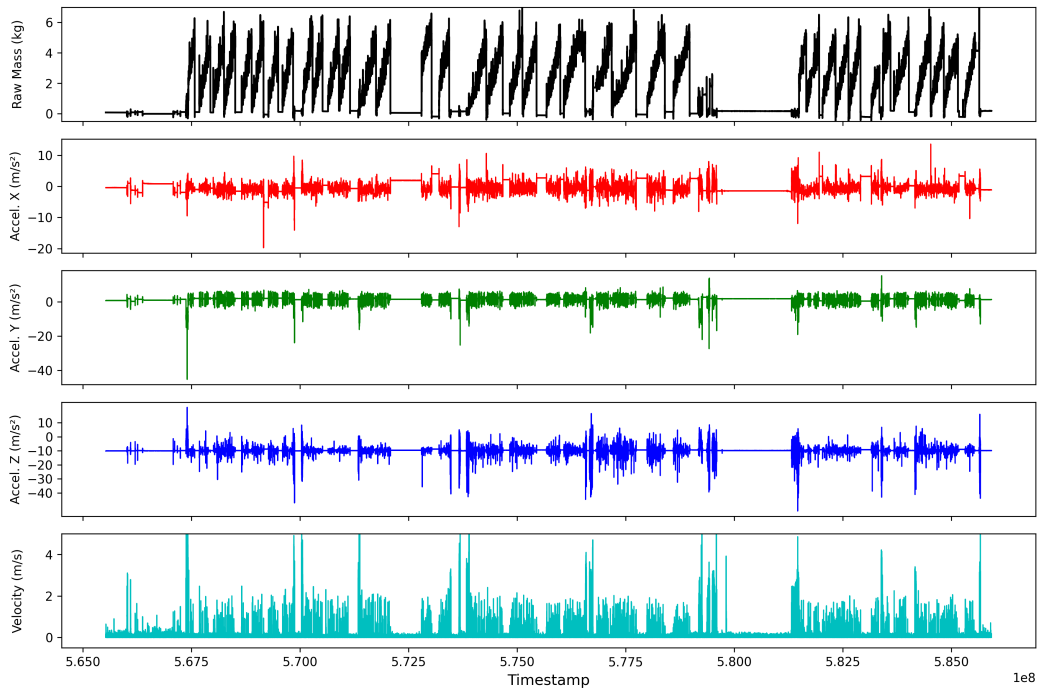


Figure 2: Time series data collected from instrumented strawberry picking carts. The plots show harvested fruit mass; acceleration along the x-axis (red), y-axis (green), z-axis (blue); and velocity (magenta). Each sawtooth structure of the mass data represents full or partially full tray mass increments over time.

velocity was derived from latitude and longitude measurements. The sawtooth-like mass signal indicates an increase in harvest mass as the picker places berries in the tray. Additionally, the periods with almost zero mass represent the times when the pickers were not picking, such as delivering a full tray to the delivery station, returning with an empty tray, switching rows with a partially full tray to continue harvesting, taking meal and personal breaks, and time before and after the harvest. The acceleration and velocity data also show the period when iCarrito was actively handled by pickers as represented by perturbations along the x, y, and z axes.

## **2.2 Overview of Picker Efficiency Estimation System**

The picker efficiency estimation consisted of two major steps: CNN-LSTM for activity recognition, followed by the picker efficiency estimation. The objective of the CNN-LSTM was to classify the harvest data into the periods when a picker was actively picking (“Pick” activity) and periods when the picker was not picking (“NoPick” activity). Once the data was classified into “Pick” and “NoPick” classes, the next step was to estimate picker efficiency. However, the “NoPick” class included all non-picking data, including the data not related to harvesting, such as the idle time before the start of the harvest, after the end of the harvest, and during the meal breaks. Hence, the “NoPick” data not related to active harvesting were excluded. Finally, the picker efficiency was estimated as the percentage of time spent picking over the entire harvest period and the amount of time required to fill up a tray.

## **2.3 CNN-LSTM for Activity Recognition**

### **2.3.1 Data annotation**

The ability of the CNN-LSTM to classify raw data depends on the manually annotated ground truth data used to train network parameters. In this study, the common approach of manual data annotation was challenging as the recorded data consisted of several million data points. Therefore, the data was annotated using a two-step approach: an automated unsupervised algorithm to label the data, followed by manual refinement with an annotation tool. Algorithm 1 illustrates the unsupervised algorithm to label the raw harvest data as “Pick” or “NoPick” label. To design the algorithm, non-picking data was identified and removed in a systematic manner. After completing all removal steps, the remaining data was then labeled as picking. In our case, identifying non-picking data was relatively straightforward. The non-picking data was related to recordings outside the field boundary, cases where mass was zero, and occurrences of noisy

location jumps that resulted from sensor limitations or from pickers handling the carts. Let the cart data be represented as  $C = \{(x_i, y_i, w_i, a_{x_i}, a_{y_i}, a_{z_i}, t_i)\}_{i=1}^N$ . Here,  $(x_i, y_i)$  is the cart's location,  $w_i$  is harvest mass, and  $(a_{x_i}, a_{y_i}, a_{z_i})$  is cart acceleration along the x, y, and z axes at the corresponding timestamp  $t_i$ . The row locations  $R = \{(r_{x_j}, r_{y_j})\}_{j=1}^M$  were measured from the RTK GPS and were used to compute the polygon to outline the field boundary defined by vertex coordinates  $F = \{(x_f, y_f)\}_{f=1}^K$ . Let  $C'$  be a modified version of the cart data  $C$ , in which non-relevant data points related to non-picking periods were systematically removed.

---

**Algorithm 1** Data Annotation for Picking Events

---

1: **Input:**

Cart data  $(C) = \{(x_i, y_i, w_i, t_i)\}_{i=1}^N$   
Field boundary coordinates  $(F) = (x_f, y_f)_{f=1}^K$

2: **Output:** Annotated data  $A$

3:  $C' \leftarrow C$

4: Define field boundary polygon:  $P \leftarrow \text{Polygon}(F)$

5: Remove data points outside the field boundary:

$$C' \leftarrow \{(x_i, y_i, w_i, t_i) \in C \mid (x_i, y_i) \in P\}$$

6: Cluster location data and remove noisy location

6.1  $C_{pos} \leftarrow (x_i, y_i, t_i)_{i=1}^N$  from  $C'$

6.2  $clusters \leftarrow \text{DBSCAN}(C_{pos}, \epsilon, minPts)$

6.3  $C' \leftarrow \{(x_i, y_i, w_i, t_i) \in C' \mid cluster_{id} \neq noise_{id}\}$

7: Remove noisy weight data:

$$C' \leftarrow (x_i, y_i, w_i, t_i) \in C' \mid w_{min} < w_i < w_{max}$$

8: Assign picking status to cart data:

$$A \leftarrow \{(x_i, y_i, w_i, t_i, \text{Pick} \leftarrow 1) \mid (x_i, y_i, w_i, t_i) \in C'\}$$

$$\cup \{(x_i, y_i, w_i, t_i, \text{NoPick} \leftarrow 1) \mid (x_i, y_i, w_i, t_i) \in C \setminus C'\}$$

9: Return  $A$

---

First, data points located outside the field boundary were removed. To accomplish this, a polygon (P) was created using the field boundary coordinates, and the data points that fell outside the polygon boundary were removed. Next, noisy location data was removed using an unsupervised clustering approach. The intuition behind this step was that the data related to the harvested tray were in the form of clusters with closely spaced cluster elements in both time and space. DBSCAN algorithm was used for data clustering, which assigned the data points to specific clusters or identified them as noise. All data points classified as noise were removed in this step. In the following step, data associated with invalid weight measurements were removed. The weight data less than the empty tray (0.5 Kg) or more than the full tray weight (5.5 Kg) was considered invalid. This step also eliminated data related to idle time, such as when the picker was delivering a full tray and returning with an empty one, time before and after the harvest, during breaks,

or an abrupt increase in weight data due to inadvertent pressure applied to the load cells from placing the trays or bumping against the bed edges. In the final step, all the remaining data in the filtered dataset  $C'$  was labeled as “Pick”, and those in the input cart data  $C$  but not in filtered data  $C'$  were labeled as “NoPick.” Once the data was annotated with the automated algorithm, the annotation was formatted in a format readable by the time-series data annotation tool Label Studio (<https://labelstud.io/>). The loaded annotation files were reviewed and updated, if necessary, manually.

### 2.3.2 CNN-LSTM architecture

The proposed CNN-LSTM model followed a hybrid architecture with a combination of CNN and LSTM models. It consisted of a U-shaped CNN feature extraction block followed by a combination of BiLSTM and LSTM layers and a final classification block (see Figure 3). The U-shaped CNN block extracted the spatial feature from the input data, while the LSTM extracted the long-term time dependencies in the harvest data. Similar to UNet, the CNN block consisted of encoder and decoder stages with skip connections for hierarchical feature extraction and transmission to the deeper layers. The encoder consisted of five encoding stages ( $e_1$  to  $e_5$ ) that progressively extracted features from the input data. Each encoder stage included  $Conv1d(C_i, C_o, k = 9, s = 1, p = \text{same})$  layers, followed by Batch Normalization, ReLU activation, and MaxPooling1D. Here,  $C_i$  and  $C_o$  were the numbers of input and output channels, and  $k$ ,  $s$ , and  $p$  were kernel size, step size, and padding, respectively. The number of output feature channels from  $e_2$  to  $e_5$  in the encoder was increased progressively from 32 to 256 (32, 64, 128, 256) while the feature dimension was decreased by factors of (8, 6, 4, 2).

The decoder section consisted of a series of upsampling and convolution layers to reconstruct the spatial features. The features extracted from the encoders were connected to the decoders at the same feature extraction level through skip connections, providing low-level features to be transmitted into the deeper layers. Each decoding stage started with a feature concatenation, upsampling, convolution [ $Conv1d(C_i, C_o, k = 9, s = 1, p = \text{same})$ ], BatchNormalization, and ReLU activation. The feature map sizes were increased by the UpSampling1D operations using the same scaling factors as the encoder’s MaxPooling1D but in reverse order: (2, 4, 6, 8). This resulted in a progressive increase in feature dimensions and a decrease in the number of channels through the decoder blocks.

After the data was processed through the CNN block, the resulting feature map was fed to the LSTM block consisting of two BiLSTM and one LSTM layer. The BiLSTM network consisted of 64 and 32 units to capture both past and future temporal contexts. The final LSTM layer was unidirectional, with 16 units.



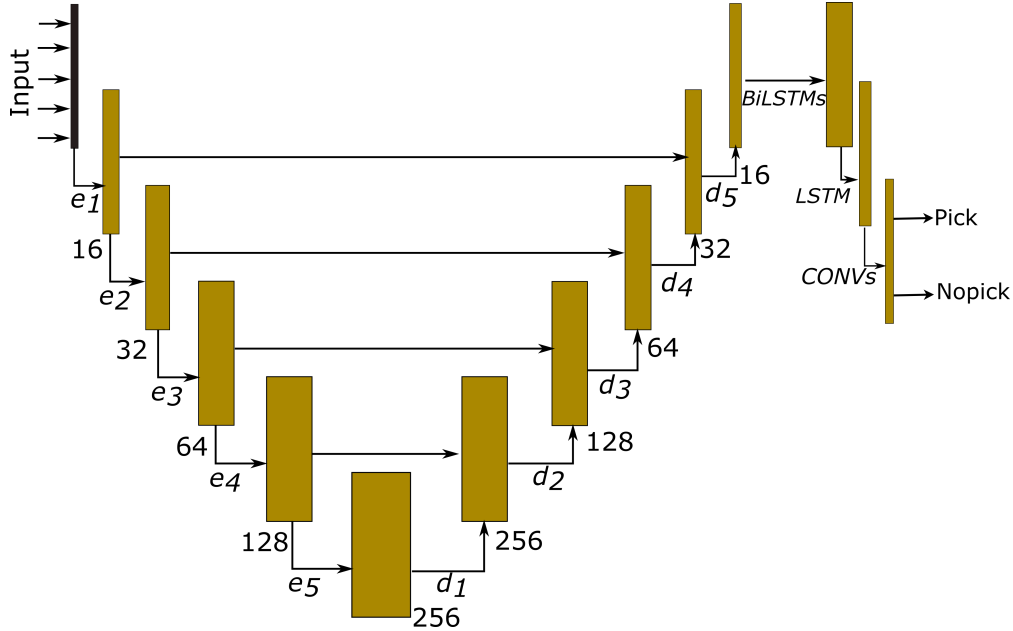


Figure 3: The CNN-LSTM architecture used for picker activity classification. The U-shaped CNN encoder-decoder extracts hierarchical spatial features, while the LSTM layers capture temporal dependencies in the time-series data. The final convolution layers distinguish between “Pick” and ‘NoPick’ activities.”

After the LSTM block, the processed data was passed to the classification block. This classification block consisted of two 1D convolutional layers. The first layer included a hyperbolic tangent activation function, followed by a second layer with a softmax activation function.

### 2.3.3 Network training details

The network was trained up to 50 epochs with a batch size of 270 using Google Colab in a GPU-accelerated environment. To optimize the model parameters, the Adam optimizer was employed with an initial learning rate of  $1 \times 10^{-3}$  and standard beta values ( $\beta_1 = 0.9$ ,  $\beta_2 = 0.999$ ). Furthermore, for our multi-class classification task, the categorical cross-entropy was used as a loss function. The network was trained using Leave-one-out Cross-Validation (LOOCV) approach in which data from one harvest day was excluded from training and reserved for testing. The remaining data was split into training and validation sets in an 80:20 ratio. Furthermore, to evaluate the impact of different input features on the classification accuracy of the network, the network was trained using five combinations of input features: i) velocity only; ii) acceleration only; iii) mass only; iv) a combination of mass and acceleration; and v) a combination of mass, acceleration, and velocity.

## 2.4 Picker Efficiency Metrics

The picker efficiency was estimated based on the classification results from the CNN-LSTM model. First, the “NoPick” data not related to harvesting were removed. The removed data were the data related to before the first and after the last “Pick” activity and the duration of breaks. The number of breaks during the harvest was manually identified from the raw data. Pickers took breaks simultaneously, and these breaks could be recognized as an extended period when the majority of carts were idle. After removing the data unrelated to harvesting, picker efficiency was calculated by estimating the percentage of time spent actively picking (Active harvest percentage) during the harvesting period and the average time to fill up a tray (Tray fill time). The active harvest percentage was calculated as:

$$\text{Active harvest percentage} = \frac{\text{Total pick time}}{\text{Total harvest time}} \times 100\% \quad (1)$$

The “Total harvest time” was the valid harvest time after excluding the idle periods before and after the harvest and during breaks, while the “Total picking time” was the cumulative time spent actively picking. Furthermore, the tray fill time was calculated as:

$$\text{Tray fill time} = \frac{\text{Total pick time}}{T} \quad (2)$$

“T” was the total number of harvested trays by a cart. The number of harvested trays was manually counted from the raw harvest data and validated by cross-referencing with the harvest tray counts provided by the grower to compensate the pickers.

### 2.4.1 Picker Efficiency Estimation from Season-long Harvest Data

The picker efficiency for season-long harvest (April 10, 2024 - July 17, 2024) was estimated by processing the entire season harvest data collected from 752 iCarritos, recording 2,962 hours of harvest data. All the data was first classified by the activity recognition algorithm, followed by efficiency estimation in terms of active harvest percentage and tray fill time. The Interquartile Range (IQR) method was used to identify and remove outliers from the harvest data by setting the outlier thresholds at 1.5 times the IQR below the first quartile and above the third quartile.

## 2.5 System Performance Evaluation

### 2.5.1 Evaluation of CNN-LSTM for activity recognition

The model performance was evaluated using a five-fold Leave-one-out Cross-Validation (LOOCV) approach. Five separate experiments were conducted where data from one harvest day was reserved for testing. The classification output for each experiment was then compared against manually annotated ground truth by computing Precision, Recall, and F1 score metrics. The final model performance was then calculated as the average of these metrics across five experiments.

### 2.5.2 Evaluation of picker efficiency estimation

To evaluate the picker efficiency estimation algorithms, the ground truth picker efficiency data was computed from the ground truth annotations used to train and evaluate the CNN-LSTM network. The data corresponding to idle time before and after the harvest and rest breaks were removed from the annotated data. The active harvest percentage and tray fill time were estimated as illustrated in equations 1 and 2. The picker efficiency estimation was evaluated by computing active harvest percentage estimation accuracy and tray fill time estimation accuracy, as given below.

$$\text{Active harvest percentage estimation accuracy} = \left( 1 - \frac{1}{C} \sum_{i=1}^C \frac{|\text{gt\_harvestpercent}_i - \text{est\_harvestpercent}_i|}{\text{gt\_harvestpercent}_i} \right) \times 100\% \quad (3)$$

$$\text{Tray fill time estimation accuracy} = \left( 1 - \frac{1}{C} \sum_{i=1}^C \frac{|\text{gt\_trayfilltime}_i - \text{est\_trayfilltime}_i|}{\text{gt\_trayfilltime}_i} \right) \times 100\% \quad (4)$$

Where  $C$  was the total number of carritos used for evaluation.

## 3 Results and Discussions

### 3.1 Evaluation of CNN-LSTM for activity recognition

Table 1 shows the average precision, recall, and F1 score of the CNN-LSTM model trained on different combinations of input training features. All the input training features showed promising results, with precision, recall, and F1 scores of more than 0.97, except for the velocity data. Using velocity as input

training data resulted in the lowest precision (0.945), recall (0.953) and F1 score (0.948), indicating that the velocity data alone may not be sufficient as a standalone harvest indicator. This limitation could be due to the fact that velocity was derived from GPS location data. Since the iCarritos relied on the low-cost GNSS unit with SBAS-based corrections, the localization accuracy may not have been sufficient to compute precise cart velocity to capture harvest-related signals. Training on acceleration data demonstrated competitive performance with a precision of 0.963 and an F1 score of 0.972, while training using only mass data achieved even better results with the highest recall (0.984) and F1 score (0.974). The combination of acceleration and mass data also showed excellent performance with high average precision (0.964), recall (0.984), and F1 scores (0.973). Finally, the combination of mass, IMU, and velocity achieved a high precision (0.966) but a low recall score (0.979), resulting in a reduced F1 score of 0.972.

Table 1: Performance metrics of the CNN-LSTM for different training feature sets

Training features	Precision	Recall	F1
vel	0.945	0.953	0.948
ax, ay, az	0.963	0.983	0.972
mass	0.965	<b>0.984</b>	<b>0.974</b>
mass, ax, ay, az	0.964	<b>0.984</b>	0.973
mass, ax, ay, az, vel	<b>0.966</b>	0.979	0.972

The results suggest that the mass and acceleration measurements captured weight change and the cart motion pattern distinctive to the picking and non-picking events. While training only with mass data showed better results, combining acceleration with mass could provide more robust results in unseen data because both sensors capture the unique contexts of the harvest. Therefore, for the purpose of picker efficiency computation, the model trained on both mass and acceleration data was used as a balance between prediction accuracy and generalizability in real-world harvesting conditions. The decrease in F1 score while combining mass, acceleration, and velocity was likely due to network overfitting and potential noise from GPS errors. The network may overfit because the feature information from velocity data may also be extracted from the IMU data, resulting in redundant training features. Figure 4 shows a visual representation of the classification results during the early and peak harvest period of the season. The upper plot shows harvest data from the beginning of the season, characterized by a higher tray-filling time (low mass slope with time) with only a few boxes harvested per day. In contrast, the lower plot represents the peak harvest season with substantially lower tray-filling times (high mass slope) and larger numbers of filled trays within the same harvest period. In Figure 4, the predicted true positives (TP) and true negatives (TN) are marked in green, while false positives (FP) and false negatives (FN) are marked in red and blue, respectively. Despite the substantial difference in tray-filling time and slope of mass data between these two phases of the season, the

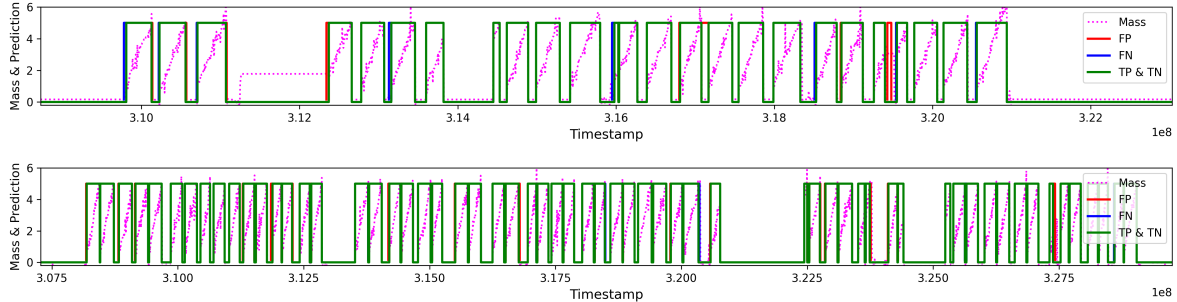


Figure 4: Classification results of picker activity recognition during early (April 24, 2024, top) and peak (May 25, 2024, bottom) periods of harvest season. The square wave-like structures represent the model predictions. True positives (TP) and true negatives (TN) are marked in green, false positives (FP) in red, and false negatives (FN) in blue color. The magenta color indicates the harvest mass over time.

developed network demonstrated robust, consistent, and promising performance.

### 3.2 Evaluation of picker efficiency estimation

Table 2: Statistical summary of picker efficiency estimation accuracy

Statistic	Active harvest percentage (%)	Tray fill time (%)
Mean	95.42	96.29
Median	96.59	97.37
Range	80.19 – 99.89	77.87 – 99.89
Standard Deviation	3.85	3.95

The picker efficiency estimation also demonstrated impressive results, with a mean and median estimation accuracy of over 95% and 96% for both the active harvest percentage and tray fill time. Table 2 presents the statistical summary, and Figure 5 provides the box plot representations of both estimation accuracies. The results showed that the developed algorithms were robust in estimating picker efficiency throughout the observed harvest period. While the mean and median accuracies were high, there were few outliers, and the results may be influenced by factors such as dataset anomalies, including sensor glitches, unusual cart movements, or the limitations of the neural network model. Nevertheless, the low standard deviation (3.95 for harvest time per tray and 3.85 for picking efficiency) indicates that estimation accuracy clustered closely around the mean with reliable results.

### 3.3 Estimation of Picker Efficiency from Season-long Harvest Data

The picker efficiency analysis on season-long harvest data showed that, on average, pickers spent 73.56% (95% CI: [73.20, 73.93]) of their total harvest time actively picking strawberries. This suggests that pickers spent approximately 26.44% of the total harvest time on non-picking activities such as traveling to and from

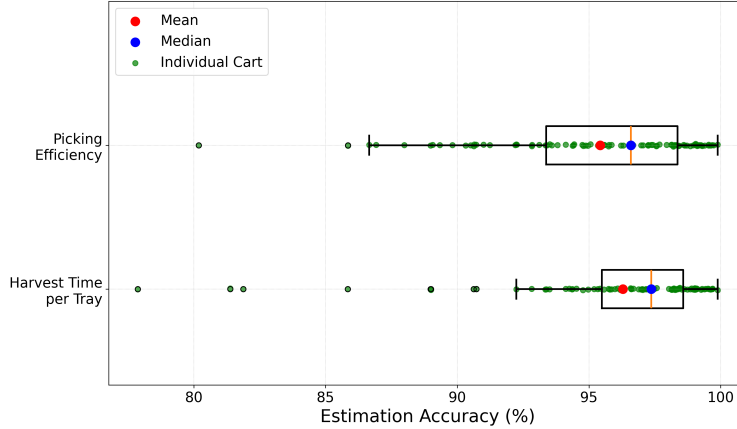


Figure 5: Box plot showing the accuracy of picking efficiency and harvest time per tray estimation. The mean and median estimation accuracy of both metrics was consistently above 95%.

the headland to deliver full trays and retrieve empty ones, waiting in delivery queues, switching between rows to continue harvesting, and taking personal or restroom breaks. Furthermore, pickers spent an average of 6.22 minutes (95% CI: [5.99, 6.45]) filling a tray, with individual tray fill times ranging from 1.84 minutes to 15.3 minutes. Table 3 presents the statistical summary of estimated picker efficiency metrics. Furthermore, Figure 6 shows the box plots and frequency distributions of the active harvest percentage and tray fill time followed by their trend over the harvest season. The frequency distribution plot (Figure 6, center) shows that approximately 40% of picker efficiency was around 75%, while approximately 72% of trays were filled within 7 minutes.

Table 3: Summary of picker efficiency estimation for season-long harvest

Statistic	Active harvest percentage (%)	Tray fill time (mins)
Mean	73.56	6.22
Median	73.96	5.09
Range	60.46 – 86.80	1.84 – 15.30
Standard Deviation	5.04	3.06
95% Confidence Interval (CI)	[73.20, 73.93]	[5.99, 6.45]

The variability in active harvest percentage may be primarily influenced by the location of the collection station in relation to the picker’s picking area and the yield of the field. Collection stations are positioned at headlands, and different pickers may need to travel different distances to deliver full trays, even though the yield was similar. Furthermore, during the early and late parts of the season, when yields were lower, pickers spent less time traveling to the collection station and more time actively harvesting, influencing the variability in picker efficiency. On the other hand, the tray fill time may have been completely influenced by yield. Higher yield results in a faster tray fill rate and vice versa. The seasonal trend (Figure 6, bottom right) indicates that tray fill times were higher at the beginning of the season due to lower yields. As the

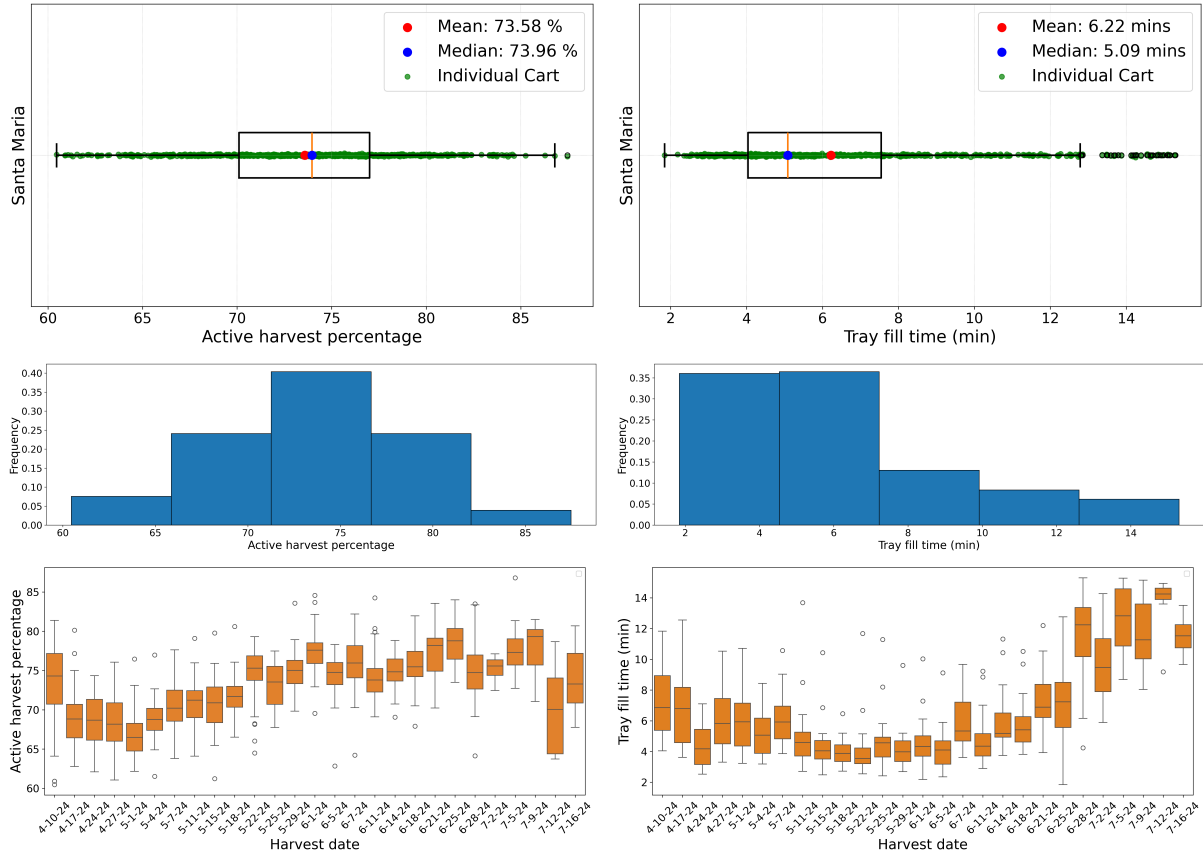


Figure 6: Seasonal picker efficiency analysis: a comprehensive analysis of picker efficiency throughout the strawberry harvest season in Santa Maria, CA. The top and middle rows show the box plots and frequency distribution of the active harvest percentage (left) and tray fill time (right). The bottom row shows the trend of the active harvest percentage (left) and tray fill time (right) from the beginning to the end of the harvest season.

season progressed and yields increased, tray fill times decreased, only to rise again towards the end of the harvest season as yields diminished.

## 4 Conclusions

In this study, an automated picker activity recognition and efficiency estimation system was developed for manual strawberry harvest using instrumented picking carts (iCarritos) and a CNN-LSTM deep learning model. Harvest data was collected using iCarritos during commercial strawberry harvests, followed by activity recognition and efficiency estimation. Based on the results of this study, the following conclusions were drawn.

- CNN-LSTM could provide robust performance for activity recognition tasks in agriculture using

time series mass and acceleration data, achieving an F1 score of more than 0.97 in classifying picker activities into “Pick” and “No Pick” categories.

- The results from the CNN-LSTM model could be post-processed to reliably estimate picker efficiency, with a mean active harvesting percentage estimation accuracy of 95.42% and tray fill time estimation accuracy of 96.29%.
- Analysis of the season-long harvest data revealed that pickers spent, on average, 73.56% of their total harvest time actively picking strawberries, with the remaining 26.44% attributed to non-picking activities. The average tray fill time was found to be 6.22 minutes.

The developed system offers a practical solution for automated worker activity monitoring in commercial strawberry fields. By providing detailed data on picker efficiency, growers can identify areas for improvement, optimize resource allocation, and enhance overall harvest efficiency. The publicly released annotated dataset further contributes to advancing research in this area.

## Acknowledgments

This work was funded by the USDA Agricultural Research Service (USDA-ARS) Non-Assistance Cooperative Agreements 58-2038-9-016 and 58-2038-3-029. We would also like to acknowledge the support of Dennis Lee Sadowski and Alejandro Torres Orozco, whose contributions are invaluable to the success of this study.

## References

- Anjom, F. K., Vougioukas, S. G., and Slaughter, D. C. (2018). Development and application of a strawberry yield-monitoring picking cart. *Computers and electronics in agriculture*, 155:400–411.
- Arad, B., Balendonck, J., Barth, R., Ben-Shahar, O., Edan, Y., Hellström, T., Hemming, J., Kurtser, P., Ringdahl, O., Tielen, T., et al. (2020). Development of a sweet pepper harvesting robot. *Journal of Field Robotics*, 37(6):1027–1039.
- Bratt, I. (2015). On u.s. farms, fewer hands for the harvest - wsj. <https://www.wsj.com/articles/on-u-s-farms-fewer-hands-for-the-harvest-1439371802>. (Accessed on 01/04/2025).
- Dabrowski, J. J. and Rahman, A. (2023). Fruit picker activity recognition with wearable sensors and machine learning. In *2023 International Joint Conference on Neural Networks (IJCNN)*, pages 1–8. IEEE.



- Fei, Z., Shepard, J., and Vougioukas, S. G. (2020). Estimation of worker fruit-picking rates with an instrumented picking bag. *Transactions of the ASABE*, 63(6):1913–1924.
- Hubbart, S. (2020). A shortage of farm guest workers could threaten america’s harvest- global trade magazine. <https://www.globaltrademag.com/a-shortage-of-farm-guest-workers-could-threaten-americas-harvest/>. (Accessed on 01/04/2025).
- Pal, A., Leite, A. C., Gjevestad, J. G., and From, P. J. (2023). A video-based activity classification of human pickers in agriculture. *arXiv preprint arXiv:2311.10885*.
- Xiong, Y., Ge, Y., Grimstad, L., and From, P. J. (2020). An autonomous strawberry-harvesting robot: Design, development, integration, and field evaluation. *Journal of Field Robotics*, 37(2):202–224.
- Zhang, K., Lammers, K., Chu, P., Li, Z., and Lu, R. (2024). An automated apple harvesting robot—from system design to field evaluation. *Journal of Field Robotics*, 41(7):2384–2400.